



SET DOMAIN GROUP 721 protein functions in saline–alkaline stress tolerance in the model rice variety Kitaake

Yutong Liu¹, Xi Chen¹, Shangyong Xue¹, Taiyong Quan², Di Cui³, Longzhi Han³ , Weixuan Cong¹, Mengting Li¹, Dae-Jin Yun^{1,4}, Bao Liu¹ and Zheng-Yi Xu^{1,*} 

¹Key Laboratory of Molecular Epigenetics of the Ministry of Education (MOE), Northeast Normal University, Changchun, P. R. China

²School of Life Science, Shandong University, Qingdao, P. R. China

³Institute of Crop Sciences, Chinese Academy of Agricultural Sciences, Beijing, P. R. China

⁴Department of Biomedical Science and Engineering, Konkuk University, Seoul, South Korea

Received 1 February 2021;

revised 7 August 2021;

accepted 10 August 2021.

*Correspondence (Zheng-Yi Xu, Tel: 86

13944933730; fax: 86 431-85099822;

email: xuzhi100@nenu.edu.cn)

Abstract

To isolate the genetic locus responsible for saline–alkaline stress tolerance, we developed a high-throughput activation tagging-based T-DNA insertion mutagenesis method using the model rice (*Oryza sativa* L.) variety Kitaake. One of the activation-tagged insertion lines, *activation tagging 7* (AC7), showed increased tolerance to saline–alkaline stress. This phenotype resulted from the overexpression of a gene that encodes a SET DOMAIN GROUP 721 protein with H3K4 methyltransferase activity. Transgenic plants overexpressing *OsSDG721* showed saline–alkaline stress-tolerant phenotypes, along with increased leaf angle, advanced heading and ripening dates. By contrast, *ossdg721* loss-of-function mutants showed increased sensitivity to saline–alkaline stress characterized by decreased survival rates and reduction in plant height, grain size, grain weight and leaf angle. RNA sequencing (RNA-seq) analysis of wild-type Kitaake and *ossdg721* mutants indicated that *OsSDG721* positively regulates the expression level of *HIGH-AFFINITY POTASSIUM (K⁺) TRANSPORTER1;5* (*OsHKT1;5*), which encodes a Na⁺-selective transporter that maintains K⁺/Na⁺ homeostasis under salt stress. Furthermore, we showed that *OsSDG721* binds to and deposits the H3K4me3 mark in the promoter and coding region of *OsHKT1;5*, thereby upregulating *OsHKT1;5* expression under saline–alkaline stress. Overall, by generating Kitaake activation-tagging pools, we established that the H3K4 methyltransferase *OsSDG721* enhances saline–alkaline stress tolerance in rice.

Keywords: *Oryza sativa* L., saline–alkaline stress, histone methylation, transcriptional regulation.

Introduction

Millions of hectares of irrigated and unirrigated agricultural land are affected by salinization and alkalization (Shahid *et al.*, 2018; Shrivastava and Kumar, 2015). Saline–alkaline soils are characterized by both high sodium ion (Na⁺) concentration and high pH, which cause more complex stress effects on plants than pH-neutral saline soils (Tang *et al.*, 2014). To survive, plants growing in saline–alkaline soils have to cope with both physiological drought and Na⁺ toxicity, in addition to the cellular damage induced by high pH (Cheng *et al.*, 2020; Liu *et al.*, 2010). Rice (*Oryza sativa* L.) serves as a staple food crop for more than half of the world population (Gross and Zhao, 2014) and as a model monocot for bioenergy research (Izawa and Shimamoto, 1996). To date, multiple mutant rice collections have been generated in different cultivars including Dong Jin, Hwayoung, Nipponbare and Zhonghua 11 (Wang *et al.*, 2013b; Wei *et al.*, 2013). Most of these mutant collections have been generated artificially through EMS mutagenesis (Henry *et al.*, 2014), irradiation (Li *et al.*, 2017; Wang *et al.*, 2013b; Wei *et al.*, 2013), T-DNA insertion (Chen *et al.*, 2003; Hsing *et al.*, 2007; Jeon *et al.*, 2000; Sallaud *et al.*, 2003; Wu *et al.*, 2003), transposon/retrotransposon insertion (van Enkevort *et al.*, 2005; Kolesnik *et al.*, 2004; Miyao *et al.*,

2003; Wang *et al.*, 2013b), RNAi (Wang *et al.*, 2013a), TALEN-based gene editing (Li *et al.*, 2012; Moscou and Bogdanove, 2009) and CRISPR/Cas9-based genome editing (Jiang *et al.*, 2013; Miao *et al.*, 2013; Xie *et al.*, 2015). Although insertion mutagenesis is an effective approach for determining the function of a genetically redundant gene, loss-of-function mutations often fail to reveal the function of a specific member of a gene family (Alonso *et al.*, 2003). Activation tagging is a powerful gain-of-function approach used to elucidate the functions of genes, especially those that exhibit high sequence similarity to other genes, a feature recalcitrant to loss-of-function genetic analyses (Gou and Li, 2011; Wan *et al.*, 2009; Weigel *et al.*, 2000). T-DNA activation tagging generates dominant mutations through the insertion of a T-DNA-carrying constitutive enhancer elements at a random position in the genome, resulting in the transcriptional activation of flanking genes (Jeong *et al.*, 2002; Memelink, 2003). This method involves the generation of a large number of transformed plants using a specialized T-DNA construct, followed by the selection of plants with the desired phenotype (Jeong *et al.*, 2006). We recently established a mutagenized population in Kitaake, a model *japonica* rice variety with a short life cycle of 9 weeks (Li *et al.*, 2016), using the activation tagging approach.

The SET domain proteins are known to methylate histone H3 at several lysine (K) residues, including H3K4, H3K9, H3K27, H3K36 and H4K20. The trithorax group (TrxG) protein family comprises a large number of functionally diverse regulatory proteins (Kingston and Tamkun, 2014), including the Su(var)3-9, Enhancer-of-zeste and Trithorax (SET) domain-containing proteins with H3K4 methyltransferase activity, ATP-dependent chromatin-remodelling factors and other associated proteins (Avramova, 2009; Krajewski *et al.*, 2005). The rice genome harbours three genes encoding TrxG family proteins, including the SET domain group protein 723 (OsSDG723; related to ATX1 and ATX2), OsSDG721 (closely related to ATX3) and OsSDG705 (related to ATX4 and ATX5) (Jiang *et al.*, 2018). Loss-of-function mutations of *OsSDG721* and *OsSDG705* in *Oryza sativa* ssp. *japonica* cv. Nipponbare caused abnormal phenotypes including semi-dwarfism, reduced cell length and reduced panicle branching (Jiang *et al.*, 2018). Moreover, genome-wide H3K4me3 levels and H3K4me3 enrichment at the gene body regions of gibberellin (GA) metabolic and signalling genes, including *SLR1*, *GID1* and *GA20 oxidases*, were reduced in the *ossdg721 ossdg705* double mutant, indicating that OsSDG721 participates in the regulation of H3K4me3 levels to control gene expression (Jiang *et al.*, 2018).

In this study, by screening the activation-tagging transgenic line collection established in Kitaake background, we identified a gain-of-function mutant, *activation tagging 7* (AC7), which showed increased tolerance to saline-alkaline stress. Thermal asymmetric interlaced PCR (TAIL-PCR) revealed that the increased tolerance to saline-alkaline stress resulted from the upregulation of the gene encoding SDG721 with H3K4 methyltransferase activity. Transgenic lines overexpressing *OsSDG721* showed saline-alkaline stress-tolerant phenotypes characterized by an increased leaf angle and advanced heading and ripening dates, whereas *ossdg721* loss-of-function mutants showed increased sensitivity to saline-alkaline stress, as indicated by the reduction in the survival rate, plant height, grain size, grain weight and leaf angle. Furthermore, *ossdg721* mutants exhibited reduced expression levels of *HIGH-AFFINITY POTASSIUM (K⁺) TRANSPORTER1;5* (*OsHKT1;5*), which was correlated with reduced H3K4me3 levels. We further showed that OsSDG721 binds to and modulates H3K4me3 levels in the promoter and coding region of *OsHKT1;5* under saline-alkaline stress.

Results

Identification of an activation-tagged rice mutant with enhanced saline-alkaline stress tolerance

To generate an activation-tagging vector, we took advantage of the *pCAMBIA1301* binary vector, which can be used for promoter trapping and activation tagging in Kitaake (Ozawa, 2009). We inserted the *green fluorescent protein (GFP)* gene driven by the maize *ubiquitin (Ubi1)* promoter between four repeats of the cauliflower mosaic virus 35S promoter ($4\times 35S$) and the $35S_{pro}$:*hygromycin* cassette (Figure 1a). This experimental design greatly facilitates the positive selection of transgenic callus generated by *Agrobacterium*-mediated transformation (Figure S1a, b). In the T2 generation, line AC7 showed increased survival rates under saline-alkaline conditions (25 mM Na₂CO₃, pH = 10.0) (Figure 1b, c). The AC7 line was backcrossed with wild-type Kitaake, followed by selfing, to

obtain the BC₁F₂ progeny, in which approximately 76% lines showed GFP signals and saline-alkaline stress tolerance (Figure S1c, d), indicating that AC7 carries a dominant mutation. To further purify the mutant genotype and to remove unwanted mutations caused by the random T-DNA insertion process (Østergaard and Yanofsky, 2004), we backcrossed line AC7 with wild-type Kitaake three more times, followed by phenotyping the BC₄F₂ progeny. Genomic sequences flanking the T-DNA insertion in line AC7 were obtained by TAIL-PCR analysis (Figure 1d). The $4\times 35S$ sequence was detected in an intergenic region on chromosome 1 containing four genes within a 10-kb sequence flanking the insertion site: *OsKitaake01g083100*, *OsKitaake01g083200*, *OsKitaake01g083300* and *OsKitaake01g083400* (Figure 1e). Transcript profiling of 4-week-old AC7 plants showed that the expression of *OsKitaake01g083200* was increased by 8-fold compared with wild-type Kitaake, whereas that of *OsKitaake01g083100*, *OsKitaake01g083300* and *OsKitaake01g083400* was unaffected (Figure 1f). Moreover, AC7 mutant plants showed increased leaf angle and advanced heading date compared with wild-type Kitaake (Figure 1g-i).

Ectopic expression of *OsSDG721* exhibits saline-alkaline stress tolerant phenotypes

To further investigate the role of *OsSDG721* in saline-alkaline stress tolerance, we generated three independent *OsSDG721* lines (*OsSDG721OX-1*, *OsSDG721OX-2* and *OsSDG721OX-3*) by cloning the *FLAG* epitope at the 3' end of the *OsSDG721* gene (Figure 2a). Real-time quantitative PCR (RT-qPCR) revealed that transcript levels of *OsSDG721* were dramatically increased in all three transgenic *OsSDG721OX* lines compared with the wild-type Kitaake (Figure 2b). Additionally, *OsSDG721OX* lines displayed saline-alkaline stress tolerant phenotypes compared with wild-type Kitaake (Figure 2c) and showed higher survival rates than wild-type Kitaake plants (Figure 2d). To examine the production of reactive oxygen species (ROS), including hydrogen peroxide (H₂O₂) and superoxide anion (O₂⁻), we stained the leaves of transgenic and wild-type plants with diaminobenzidine (DAB) and nitrotertrazolum blue chloride (NBT). The results showed lower levels of ROS in *OsSDG721OX* lines than in wild-type Kitaake (Figure 2e). Additionally, *OsSDG721OX* lines showed an increased leaf angle and advanced heading dates compared with wild-type Kitaake (Figure S2). Taken together, these results indicate that *OsSDG721* is required for saline-alkaline stress tolerance and plays an important role in plant growth and development.

Tissue-specific expression patterns of *OsSDG721*, and subcellular localization analysis of *OsSDG721*

To examine the spatial and temporal expression patterns of *OsSDG721*, we generated transgenic plants expressing the β -glucuronidase (*GUS*) gene under the control of the *OsSDG721* promoter (*OsSDG721_{pro}:GUS*) and examined the activity of the *OsSDG721* promoter in different tissues at distinct developmental stages. *GUS* signals were detected in the leaf, leaf sheath, panicle, glume, root and stem tissues (Figure S3a). These results were also confirmed by RT-qPCR (Figure S3b). Additionally, levels of *OsSDG721* transcripts and the encoded protein rapidly increased upon exposure to saline-alkaline conditions (25 mM Na₂CO₃, pH = 10.0) for 2 and 4 h but decreased after recovery (Figure S3c, d). The stress-

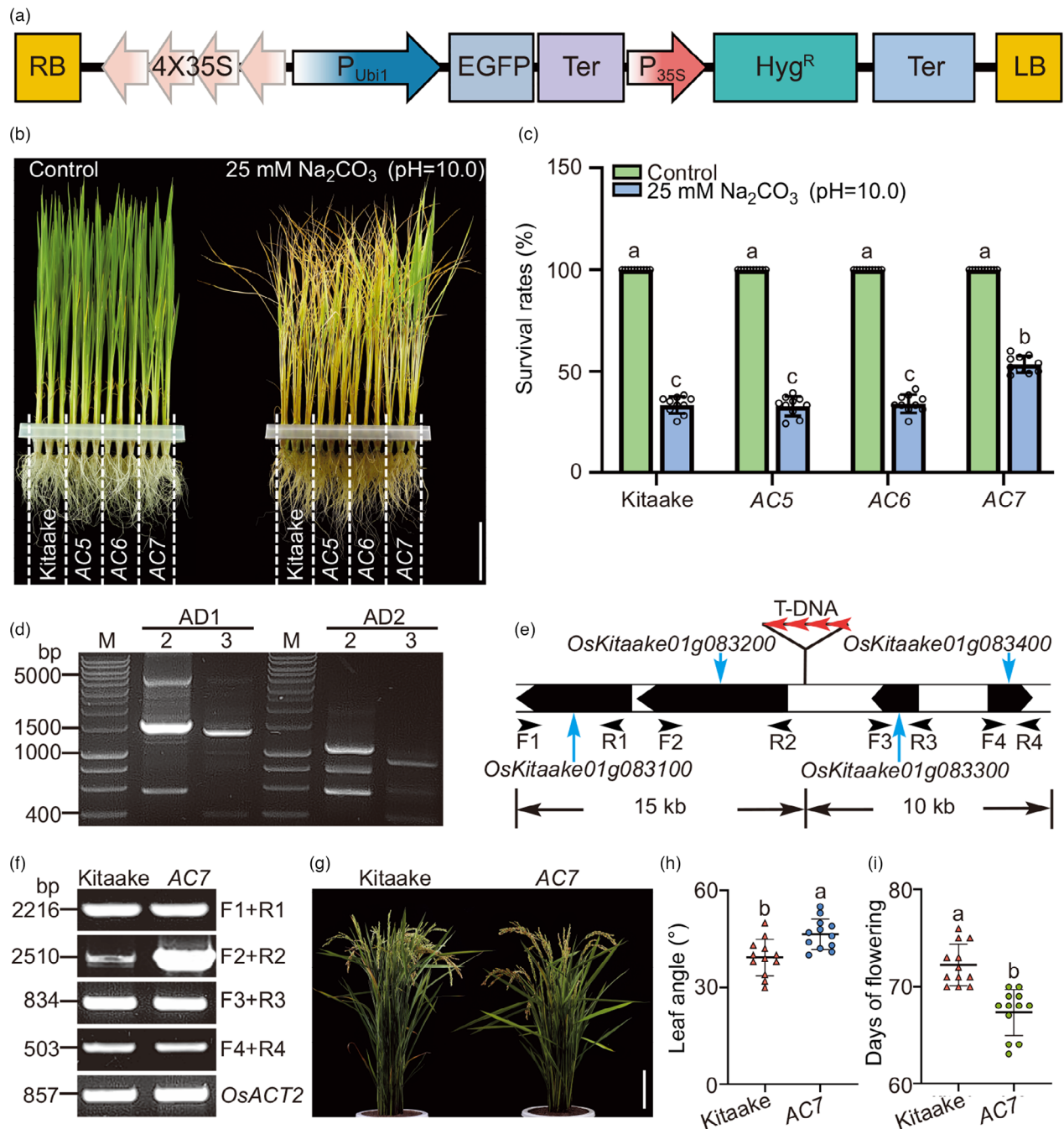
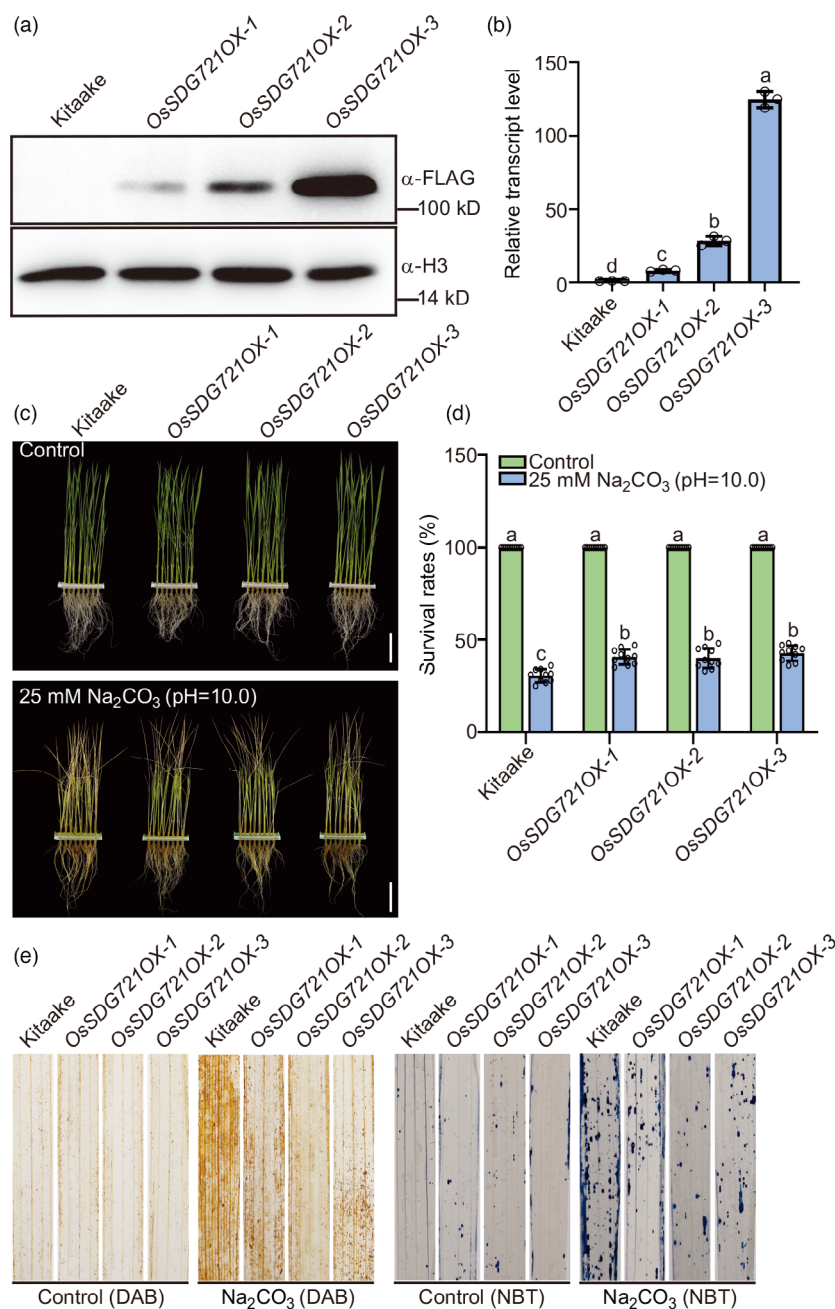


Figure 1 Isolation of saline-alkaline stress-tolerant activation tagging line, AC7. (a) Schematic representation of the vector used to generate activation tagging lines in Kitaake. RB, right border; 4×35S, four repeats of the cauliflower mosaic virus (CaMV) 35S promoter; *P_{35S}*, CaMV 35S promoter; EGFP, enhanced green fluorescent protein; *P_{Ubi1}*, maize *Ubiquitin1* promoter; *Ter*, *nopaline synthase* (*NOS*) terminator; *Hyg^R*, hygromycin resistance gene; LB, left border. (b, c) Images (b) and survival rates (c) of Kitaake, AC5, AC6 and AC7 plants before and after recovery from saline-alkaline stress treatment (25 mM Na₂CO₃, pH = 10.0). In (b), scale bar = 4 cm. Data in (c) represent mean ± standard deviation (SD) of three biological replicates, each containing 10 plants. Black circles represent the values of individual plants. Significant differences between wild-type Kitaake and AC plants were evaluated by two-way analysis of variance (ANOVA), followed by Tukey's multiple comparison test. (d) Identification of the T-DNA insertion site by thermal asymmetric interlaced PCR (TAIL-PCR). AD, arbitrary degenerate primer; 2, secondary PCR products; 3, tertiary PCR products. (e) Schematic representation of the genomic DNA flanking the T-DNA insertion site. (f) Semi-quantitative RT-PCR analyses using different primer sets. *OsACT2* served as a loading control. (g) Photographs of 90-d-old Kitaake and AC7 plants grown in field. Scale bar = 15 cm. (h, i) Quantification of agronomic traits including leaf angle (h) and flowering time (i) in Kitaake and AC7 plants. Data represent mean ± SD of three biological replicates, each containing 12 plants. Significant differences between Kitaake and AC7 plants were evaluated by one-way ANOVA, followed by Tukey's multiple comparison test.

Figure 2 Characterization of *OsSDG721* overexpression (*OsSDG721OX*) lines. (a) Immunoblot analysis of the *OsSDG721*-FLAG protein in Kitaake, *OsSDG721OX-1*, *OsSDG721OX-2* and *OsSDG721OX-3* plants using anti-FLAG antibody. Histone H3 was used as a loading control. (b) RT-qPCR analysis of *OsSDG721* transcript levels in Kitaake, *OsSDG721OX-1*, *OsSDG721OX-2* and *OsSDG721OX-3* plants. Significant differences between Kitaake and OX lines were evaluated by one-way ANOVA, followed by Tukey's multiple comparison test. (c, d) Images (c) and survival rates (d) of Kitaake, *OsSDG721OX-1*, *OsSDG721OX-2* and *OsSDG721OX-3* plants before and after recovery from the saline-alkaline stress treatment (25 mM Na₂CO₃, pH = 10.0). In (c), scale bar = 6 cm. Data in (d) represent mean \pm SD of three biological replicates, each containing 10 plants. Black circles represent the values of individual plants. Significant differences between Kitaake and OX lines were evaluated by two-way ANOVA, followed by Tukey's multiple comparison test. (e) Accumulation of reactive oxygen species (ROS) in the leaves of rice seedlings treated with or without 25 mM Na₂CO₃ (pH = 10.0). After 24 h, seedlings were stained with nitroterrazolium blue chloride (NBT) and diaminobenzidine (DAB) staining to assess the levels of O₂⁻ and H₂O₂, respectively. Three biological replicates were performed, each containing 20 seedlings.



responsive gene *OsKitaakee01g425100* gene was used as a positive control (Figure S3c) in the RT-qPCR analysis, and H3 was used as a loading control in the immunoblotting analyses (Figure S3d).

To examine the subcellular localization of *OsSDG721*, we cloned the *GFP* gene at the 3' end of the *OsSDG721* coding sequence (CDS). The *OsSDG721-GFP* construct or *GFP* alone (empty vector) was co-transfected into rice protoplasts along with the *NLS-RFP* construct, a nucleus localization maker. Green fluorescence signals co-localized with red fluorescence in protoplasts co-transformed with *OsSDG721-GFP* and *NLS-RFP* but were exclusively localized in the cytosol in protoplasts co-transformed with *GFP* and *NLS-RFP* (Figure S3e). These results indicate that *OsSDG721* localizes to the nucleus.

Loss-of-function *ossdg721* mutants exhibit saline-alkaline stress sensitive phenotypes

To confirm the role of *OsSDG721* in saline-alkaline tolerance, we generated three independent *ossdg721* loss-of-function mutants (*ossdg721-1*, *ossdg721-2* and *ossdg721-3*) using the CRISPR/Cas9 system. Single guide RNA (sgRNA) target sites for *OsSDG721* were cloned into the CRISPR/Cas9 vector (Figure S4a), in which *Cas9* was driven by the *UBQ10* promoter (Ma *et al.*, 2015). The vectors were then transformed into Kitaake plants, and homozygous *ossdg721-1*, *ossdg721-2* and *ossdg721-3* mutant lines were identified via Sanger sequencing (Figure S4b). The *ossdg721-1* and *ossdg721-2* mutants carried a 1-bp insertion of either A or T located 60 bp downstream of the transcription

start site (ATG), which resulted in a frameshift mutation and consequently a premature stop codon before the core SET domain, and the *ossdg721-3* mutant contained a 2-bp insertion at the same location, causing a frameshift (Figure S4b). To exclude the potential confounding effect of the *Cas9* gene *per se* on the plant phenotype, we selected *ossdg721-1*, *ossdg721-2* and *ossdg721-3* mutant plants for hygromycin sensitivity (Figure S4c).

To further confirm whether the loss-of-function mutation of *OsSDG721* was responsible for saline–alkaline stress sensitivity, we generated complementation lines by expressing FLAG epitope-tagged *OsSDG721* under the control of the *OsSDG721* promoter (*OsSDG721_{pro}::OsSDG721-FLAG*) in the *ossdg721-1* mutant. Two independent complementation lines (*Com#1* and *Com#2*) were chosen for further analysis, and the level of *OsSDG721-FLAG* protein in these lines was detected using Western blot analysis (Figure S4d). Both *Com#1* and *Com#2* lines showed similar survival rates compared with wild-type Kitaake plants under saline–alkaline stress (Figure 3a, b). Furthermore, staining leaves with DAB and NBT revealed increased ROS accumulation in *ossdg721* mutants (Figure 3c, d), probably because high salt and pH reduce the photosynthetic rates, leading to increased production of ROS production including H_2O_2 and O_2^- (Sharma *et al.*, 2012). Notably, *ossdg721* mutants showed no significant changes under normal conditions. Next, we examined the contents of Na^+ and K^+ in shoots and roots of Kitaake, *ossdg721* mutants and complementation lines under saline–alkaline stress. K^+ and Na^+ contents in shoots or roots did not differ significantly among the genotypes tested under normal conditions (Figure 3e, f, Figure S5). However, after treatment with saline–alkaline stress (25 mM Na_2CO_3 , pH = 10.0) for 5 d, the shoot K^+ content of *ossdg721* mutants decreased dramatically compared with that of wild-type Kitaake and complementation lines (Figure 3e), whereas the shoot Na^+ content of *ossdg721* mutants increased significantly compared with that of wild-type Kitaake and complementation lines (Figure 3f). By contrast, in roots, the Na^+ content of *ossdg721* mutant lines was only slightly higher than that of wild-type Kitaake and complementation lines, and the K^+ content showed no significant differences among the *ossdg721* mutants, wild-type Kitaake and complementation lines (Figure S5). This result implies that the loss-of-function mutation of *OsSDG721* perturbs the K^+/Na^+ ratio in shoots.

We further isolated nuclei from wild-type Kitaake and *ossdg721* mutants to determine the histone modification status in these genotypes. H3K4me3 levels were reduced in the three *ossdg721* mutants compared with that in Kitaake, whereas H3K4me1 and H3K4me2 levels were not altered (Figure S6), which is consistent with previous reports (Jiang *et al.*, 2018). In addition to the saline–alkaline stress tolerant phenotype, *ossdg721* mutants also showed a slight reduction in plant height, grain size, grain weight and leaf angle (Figure 4a–h). Together, these results indicate that *OsSDG721* is not only involved in saline–alkaline stress tolerance but also controls grain yield and crop architecture.

***OsSDG721* enhances saline–alkaline stress response by upregulating *OsHKT1;5* expression**

To explore the effect of *OsSDG721* on the genome-wide transcriptional landscape, we conducted RNA sequencing (RNA-seq) analysis of wild-type Kitaake and *ossdg721-1* plants. Genes showing differential expression were identified in shoots and

roots of rice seedlings between 0-h vs. 6-h saline–alkaline stress treatments via stringent statistical analysis of RNA-seq data (see Experimental Procedures for details). Data shown in Figure S7a, b indicate that *OsSDG721* dictates transcriptional reprogramming under normal and saline–alkaline stress conditions (Tables S1–S4). Venn diagram analysis revealed that 10,112 and 10,150 genes were regulated under saline–alkaline conditions in Kitaake shoots and roots, respectively (Figure S7c, Table S5). Comparison of the differentially expressed genes (DEGs) between Kitaake and *ossdg721-1* showed that 1213 and 1705 overlapping genes responded to saline–alkaline stress in shoots and roots, respectively (Figure S7c, Table S6), which implies that the expression of these genes is affected by *OsSDG721* under saline–alkaline stress. These saline–alkaline stress-responsive genes included *OsHKT1;5*, *OsHKT2;1* and *OsHKT1;4*. The HKT family proteins are involved in Na^+ and K^+ transport and homeostasis maintenance in many plant species (Hauser and Horie, 2010; Horie *et al.*, 2009; Munns and Tester, 2008). Intriguingly, among the DEGs identified in this study, the expression of *OsHKT1;5*, located at the salt tolerance quantitative trait locus (QTL) *SHOOT K⁺ CONCENTRATION* (*SKC1*), was dramatically reduced in mutant roots, whereas that of *OsHKT2;1*, which encodes a plasma membrane-localized subfamily II protein involved in Na^+ uptake, was dramatically induced in mutant roots (Figure S7d). Given that *OsSDG721* exhibits H3K4me3 methyltransferase activity and thus acts as a transcriptional activator, we deduced that the loss-of-function mutation of *OsSDG721* reduces the expression of *OsHKT1;5*. To further examine the genetic interaction between *OsSDG721* and *OsHKT1;5*, we generated *ossdg721 oshkt1;5* double mutants using the CRISPR/Cas9 technology. Because *OsSDG721* and *OsHKT1;5* are genetically linked, we introduced CRISPR/Cas9 constructs harbouring two sgRNA target sites for *OsHKT1;5* in the *ossdg721-1* mutant background (Figure 5a). Two double mutant lines were generated: *ossdg721-1 oshkt1;5-c1* and *ossdg721-1 oshkt1;5-c2*; the former carried a 2-bp deletion located 83 bp downstream of ATG, and the latter contained a 7-bp deletion located 194 bp downstream of the ATG (Figure 5b). Sequence deletion in both double mutants resulted in a frameshift and, consequently, a premature stop codon (Figure 5b). We also generated *oshkt1;5* single mutants in wild-type Kitaake background using a CRISPR/Cas9 construct harbouring one of the sgRNA target sites. The *oshkt1;5-c3* single mutant harboured a 2-bp deletion located 194 bp downstream of ATG, causing a frameshift and, consequently, a premature stop codon (Figure 5b). The *ossdg721-1 oshkt1;5-c1*, *ossdg721-1 oshkt1;5-c2* and *oshkt1;5-c3* mutants were screened for non-hygromycin resistance (Figure 5c). The saline–alkaline stress sensitivity of both double mutants was comparable with that of the single mutant, based on survival rates (Figure 5d, e). Moreover, no significant differences in shoot K^+ and Na^+ contents were detected among the three mutants (Figure 5f, g). These results imply that *OsHKT1;5* acts downstream of *OsSDG721*, and reduced *OsHKT1;5* expression in the *ossdg721* mutant background contributes to saline–alkaline stress sensitivity.

***OsSDG721* regulates the saline–alkaline stress response via the regulation of H3K4me3 levels at the *OsHKT1;5* chromatin**

To test whether *OsSDG721* impacts the H3K4me3 level under the saline–alkaline stress condition, we treated 2-week-old wild-type Kitaake and *ossdg721* seedlings with 25 mM Na_2CO_3 (pH = 10.0) for 0 or 6 h and examined the H3K4me3 levels by quantitative

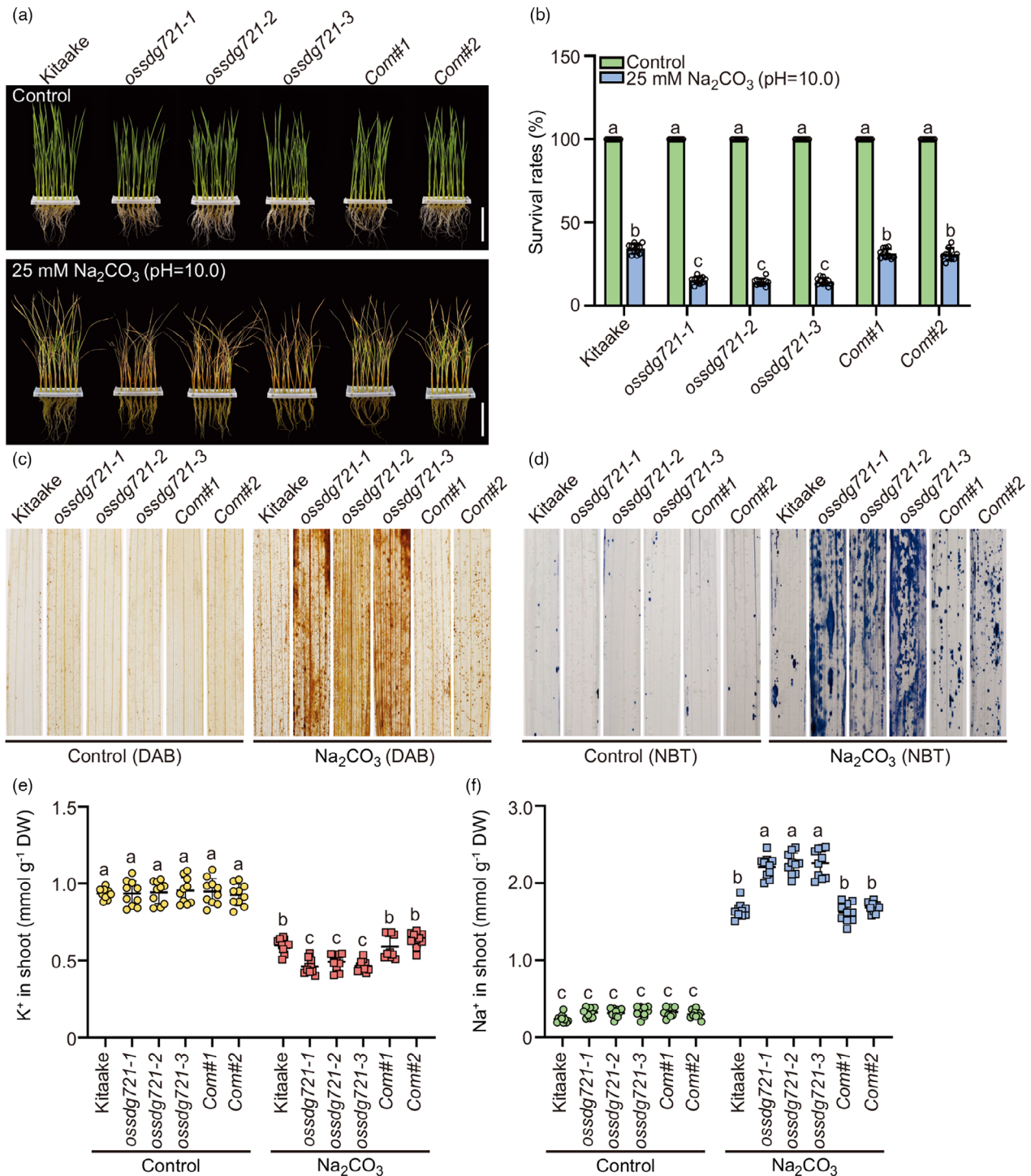


Figure 3 Characterization of loss-of-function *ossdg721* mutants under saline-alkaline stress conditions. (a, b) Images (a) and survival rates (b) of Kitaake, loss-of-function mutants (*ossdg721-1*, *ossdg721-2*, *ossdg721-3*) and complementation lines (*Com#1* and *Com#2*) before and after recovery from the saline-alkaline treatment (25 mM Na_2CO_3 , pH = 10.0). In (a), scale bar = 8 cm. In (b), data represent mean \pm SD of three biological replicates, each containing 10 plants. Black circles represent the values of individual plants. Significant differences between Kitaake and other genotypes were evaluated by two-way ANOVA, followed by Tukey's multiple comparison test. (c, d) DAB (c) and NBT (d) staining of seedlings treated with or without 25 mM Na_2CO_3 (pH = 10.0). Three biological repeats were performed for each treatment, with 20 plants per treatment. (e, f) Plots showing K^+ (e) and Na^+ (f) contents of shoots of 4-week-old seedlings of the indicated genotypes treated with or without 25 mM Na_2CO_3 (pH = 10.0) for 5 d ($n = 10$ plants per genotype). Significant differences between Kitaake and other genotypes were evaluated by two-way ANOVA, followed by Tukey's multiple comparison test. DW, dry weight.

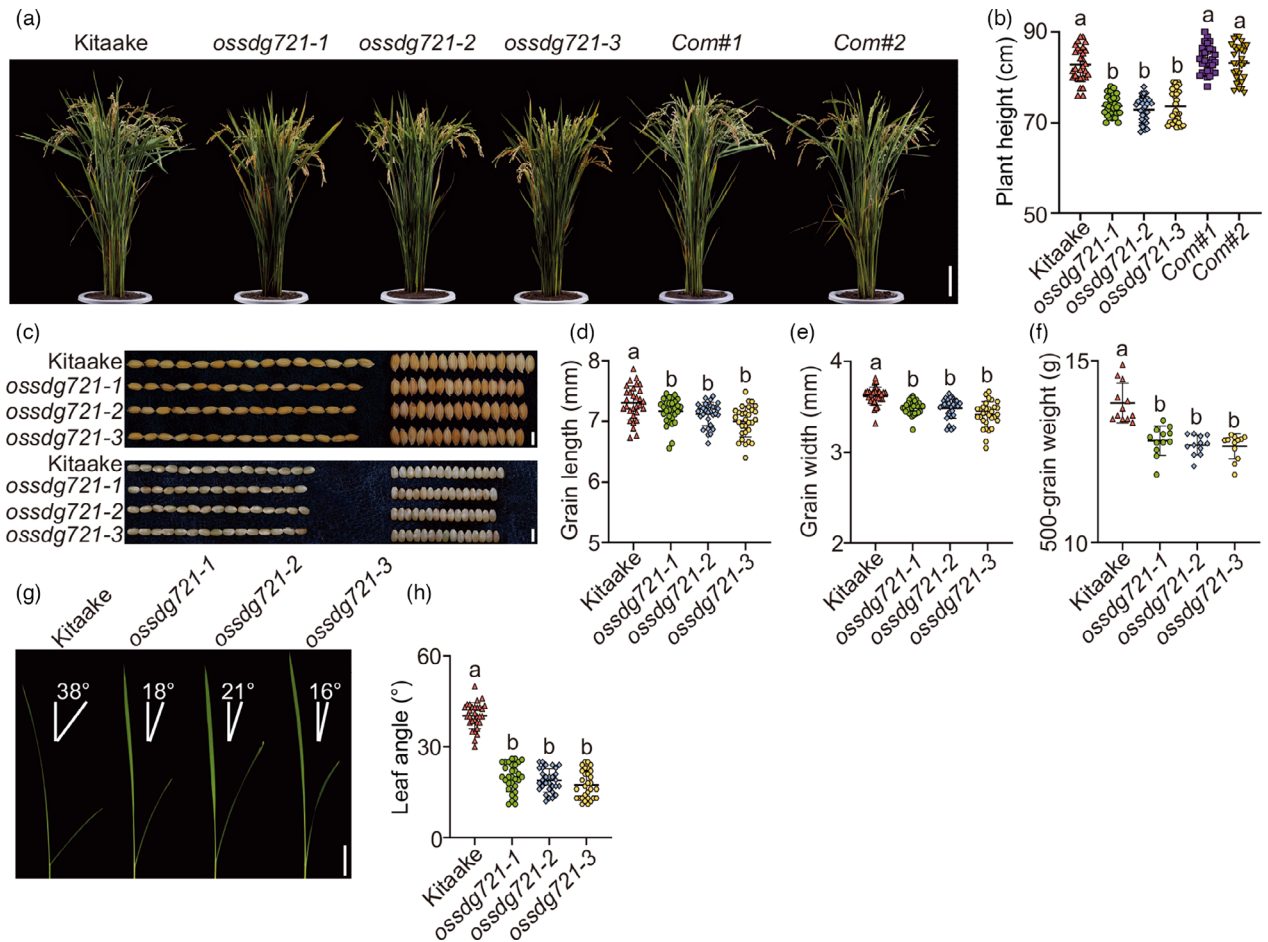


Figure 4 Phenotypes of *ossdg721* mutants and complementation lines. (a) Photographs of 90-d-old Kitaake, *ossdg721-1*, *ossdg721-2*, *ossdg721-3*, Com#1 and Com#2 plants. Scale bar = 15 cm. (b) Plant height of the each indicated genotypes. Data represent mean \pm SD ($n = 25$ plants per genotype). (c) Images of grains of the indicated genotypes. Scale bar = 7 mm. (d, e) Measurements of grain length (d) and grain width (e) of the indicated genotypes. Data represent mean \pm SD of three biological experiments, each containing 25 grains. (f) Measurement of 500-grain weight of each genotype. Data represent mean \pm SD of 12 biological experiments, each containing 500 grains. (g, h) Images (g) and quantification (h) of leaf angles of 20-d-old plants. In (g), scale bar = 3 cm. In (h), data represent mean \pm SD of three biological experiments, each containing 25 plants. Different lowercase letters represent statistically significant differences ($P < 0.05$; one-way ANOVA, followed by Tukey's multiple comparison test).

PCR (ChIP-qPCR). The result showed no significant difference in H3K4me3 levels between Kitaake and *ossdg721* seedlings under normal conditions; however, under saline-alkaline stress conditions, the increase in H3K4me3 levels was dramatically impaired in *ossdg721* seedlings compared with wild-type Kitaake seedlings (Figure 6a). Comparable changes were not detected in chromatin at the *OsUBQ10* locus, a negative control (Figure 6b). To further test whether OsSDG721 associates with the *OsHKT1;5* chromatin, we took advantage of the complementation lines (*OsSDG721_{pro}::OsSDG721-FLAG*) to perform ChIP-qPCR analysis using anti-FLAG antibody. The results showed that OsSDG721-FLAG specifically associated with the promoter and gene body of *OsHKT1;5* (Figure 6c, d). Furthermore, after 25 mM Na_2CO_3 (pH = 10.0) treatment, the association of OsSDG721-FLAG with *OsHKT1;5* chromatin increased in the complementation lines compared with Kitaake seedlings. Taken together, these results indicate that OsSDG721 binds to the *OsHKT1;5* chromatin and modulates its H3K4me3 levels. OsSDG721 established a peak level of H3K4me3-modified nucleosomes nearly 300 bp

downstream of the transcriptional start site (TSS) of *OsHKT1;5*. To further evaluate whether OsSDG721 directly binds to DNA, we performed EMSA using synthetic probes representing six different loci located in close proximity to this region. However, OsSDG721 did not bind to any of these probes (Figure S8), indicating that OsSDG721 does not exhibit DNA-binding activity. GST and OsMYB106 proteins were used as negative and positive controls for the *OsHKT1;5* promoter, based on the previous report (Wang et al., 2020).

Discussion

In this study, we generated an activation-tagged mutant pool in Kitaake, a model rice variety. This experimental design greatly facilitates the positive selection of transformed calli and is also very useful for determining whether the activation-tagged mutants are gain-of-function or loss-of-function mutants. Approximately 500 activation-tagged insertion lines were screened in this study, of which approximately 8% showed saline-alkaline stress-sensitive

or -resistant phenotypes. Using this system, we identified a gain-of-function mutant, *AC7*, which showed enhanced saline–alkaline stress tolerance compared with the wild type. Genetic and physiological analyses of line *AC7* confirmed that *OsSDG721*

positively impacts saline-alkaline stress tolerance in rice. Moreover, agronomic traits were negatively impacted in loss-of-function *ossdg721* mutants, as evident from the reduction in plant height, grain size, grain weight and leaf angle but enhanced

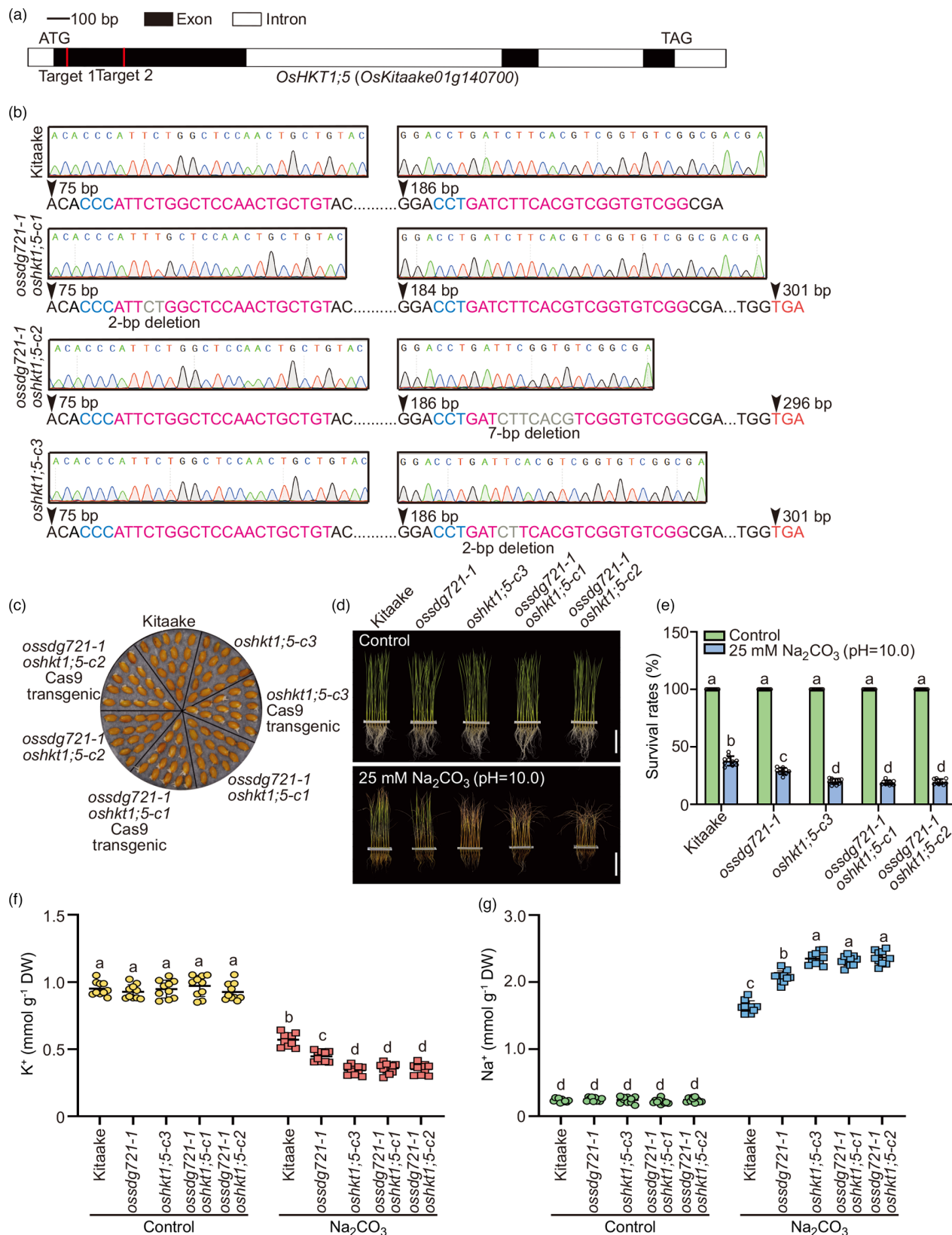


Figure 5 *OsHKT1;5* acts downstream of *OsSDG721* under saline–alkaline stress conditions. (a, b) Sequence chromatograms showing mutations induced in the *OsHKT1;5* gene in the *ossdg721-1 oshkt1;5-c1*, *ossdg721-1 oshkt1;5-c2* and *oshkt1;5-c3* mutants using the CRISPR/Cas9 technology (a), as revealed by Sanger sequencing (b). (c) Isolation of Cas9-free mutants. Plants of indicated genotypes were selected via hygromycin resistance. (d, e) Images (d) and survival rates (e) of Kitaake, *ossdg721-1*, *oshkt1;5-c3*, *ossdg721-1 oshkt1;5-c1* and *ossdg721-1 oshkt1;5-c2* plants before and after recovery from the saline–alkaline stress treatment (25 mM Na₂CO₃, pH = 10.0). In (d), scale bar = 12 cm. In (e), data represent mean \pm SD of three biological experiments, each containing 10 plants. Black circles represent the values of individual plants. (f, g) Plots showing K⁺ (f) and Na⁺ (g) contents of the shoots of 4-week-old seedlings of the indicate genotypes treated with or without 25 mM Na₂CO₃ (pH = 10.0) for 5 d (n = 10 plants per genotype). DW, dry weight. Different lowercase letters represent statistically significant differences (P < 0.05; two-way ANOVA, followed by Tukey's multiple comparison test).

in *OsSDG721OX* lines, which showed an increased leaf angle and advanced heading and ripening dates compared with wild-type Kitaake. Previously, in the *japonica* rice cultivar Nipponbare, loss-of-function mutations in *SDG721* and *SDG705* genes resulted in gibberellic acid (GA)-deficient phenotypes, including reduced cell length, semi-dwarfism and reduced panicle branching (Jiang et al., 2018). Thus, although we used a different background (Kitaake) in this study, our results were similar to those obtained by Jiang et al.

(2018) in Nipponbare. RNA-seq data analysis showed that *OsKitaake07g154900* (*OsSPL13*) and *OsKitaake09g157800* (*OsSPL18*) were downregulated in *ossdg721-1* shoots. In previous studies, *osspl18* and *osspl13* knockout mutants exhibited reduced grain width and thickness (Si et al., 2016; Yuan et al., 2019). Furthermore, *OsKitaake03g264900* (*OsIAA12*) was downregulated in the *ossdg721-1* mutant, in which the overexpression of *OsIAA12* increased the leaf inclination angle (Chen et al., 2018). It

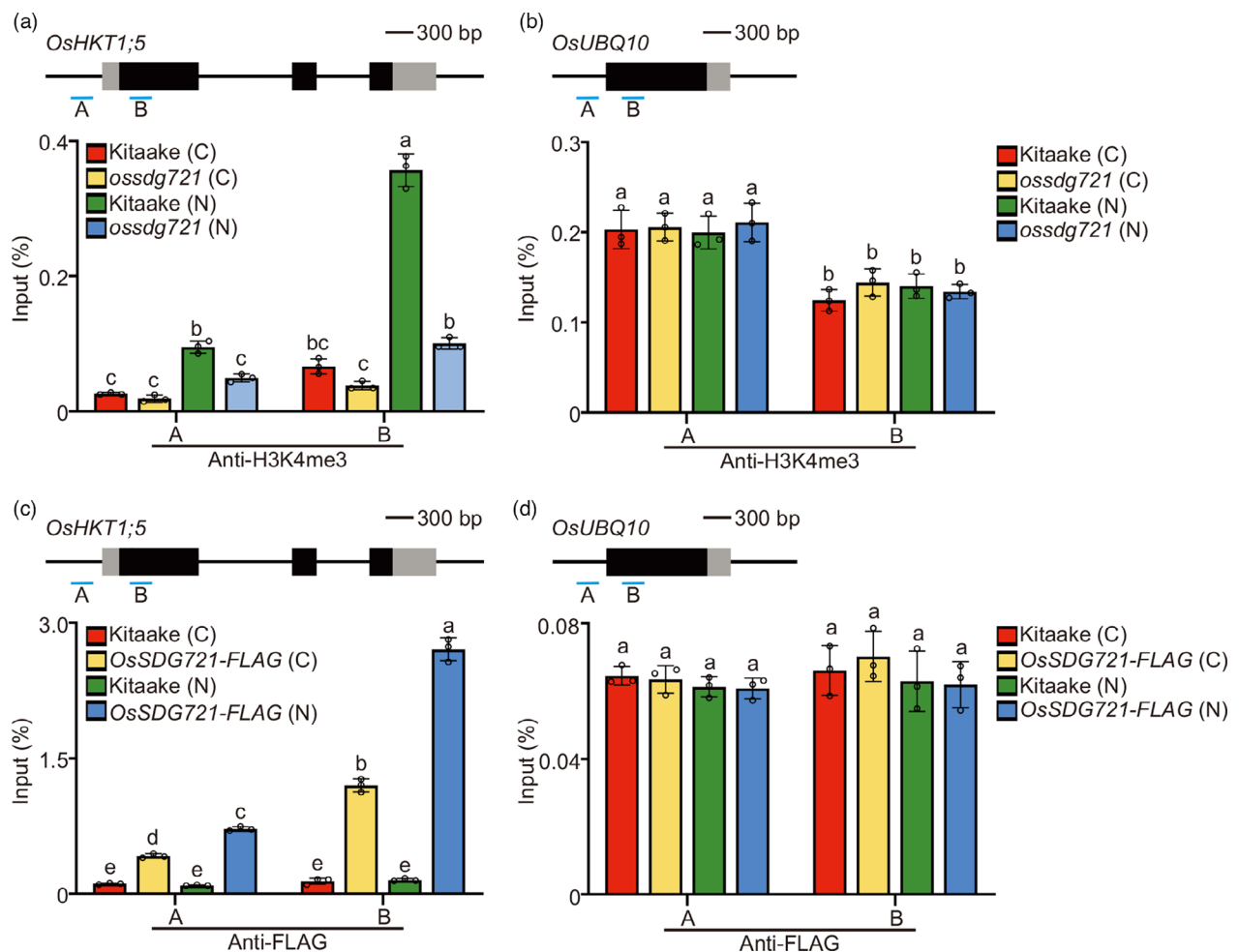


Figure 6 *OsSDG721* regulates saline–alkaline stress tolerance via the regulation of histone H3 lysine 4 trimethylation (H3K4me3) status of *OsHKT1;5*. (a, b) *OsSDG721* regulates H3K4me3 levels at *OsHKT1;5* (a) but not at *OsUBQ10* (b) under saline–alkaline stress conditions, as shown by chromatin immunoprecipitation, followed by quantitative PCR (ChIP–qPCR) using anti-H3K4me3 antibody. The X-axis denotes the genomic regions of *OsHKT1;5* (a) and *OsUBQ10* (b). Data represent mean \pm SD (n = 3). (c, d) *OsSDG721* associates with *OsHKT1;5* (c) but not with *OsUBQ10* (d), as shown by ChIP–qPCR using anti-FLAG antibody. The X-axis denotes the genomic regions of *OsHKT1;5* (c) and *OsUBQ10* (d). C, control conditions; N, Na₂CO₃ (pH = 10.0) treatment conditions. Black boxes and grey boxes represent exon and untranslated regions (UTR), respectively. Data represent mean \pm SD (n = 3). Different lowercase letters represent statistically significant differences (P < 0.05; two-way ANOVA, followed by Tukey's multiple comparison test).

is possible that altering the impact of OsSDG721 on these genes explains the changes in agronomic traits to some extent. Previous studies indicate that the SET DOMAIN GROUP proteins affect different agronomic traits in rice. For instance, OsSDG708 impacts flowering time by controlling the H3K36 methylation status of key flowering regulatory genes including *Heading date 3a (Hd3a)*, *RICE FLOWERING LOCUS T1 (RFT1)* and *Early heading date 1 (Ehd1)* (Liu *et al.*, 2016); OsSDG701, which catalyses H3K4 methylation and plays an important role in sporophyte development and sporophyte-to-gametophyte transition (Liu *et al.*, 2017). OsSDG724 modulates H3K36 methylation levels and regulates *Ehd1*, *OsMADS50* and *RFT1* expression (Sun *et al.*, 2012); OsSDG714, which governs the H3K9 methylation status of chromatin, plays important roles in regulating trichome formation and CpG and CNG cytosine methylation at the *Tos17* locus (Ding *et al.*, 2007). Although SDG proteins exhibit different histone modification specificities, some of them play overlapping functions. Thus, further studies are needed to understand how different SDG proteins coordinate to regulate plant growth and development in rice.

Intriguingly, we found that the shoot K^+ content of *ossdg721* mutant lines was reduced, whereas the shoot Na^+ content was elevated, indicating that OsSDG721 is involved in the maintenance of K^+ and Na^+ homeostasis. Furthermore, genome-wide transcriptional analysis revealed that OsSDG721 impacts the expression of *OsHKT1;5*, which was identified as the *SKC1* locus. ChIP-qPCR analysis revealed that OsSDG721 binds to the *OsHKT1;5* chromatin and controls the H3K4me3 level at this locus. According to previous reports (Lu *et al.*, 2013), OsSDG721 contains highly conserved domains, including PWWP, FYRNC, plant homeodomain (PHD) and SET. Among these domains, only PWWP exhibits nucleosome-binding capability (Lu *et al.*, 2013). Moreover, a recent study demonstrated that the PWWP domain of mouse Dnmt3a exhibits little DNA-binding activity, in contrast to Dnmt3b, which binds to DNA in a non-sequence-specific manner (Chen *et al.*, 2004). As OsSDG721 also harbours the PWWP domain, we tested whether OsSDG721 also binds to DNA in a sequence-specific or non-sequence-specific manner. However, our results showed that OsSDG721 does not bind to the *OsHKT1;5* promoter or region downstream of the TSS. Recent studies revealed that a transcriptional regulatory complex composed of BCL2-ASSOCIATED ATHANOGENE4 (OsBAG4), OsMYB106 and OsSUVH7 regulates *OsHKT1;5* expression in response to salt stress. OsMYB106 and OsSUVH7 bind to the MYB binding *cis*-element (MYBE) in the *OsHKT1;5* promoter and to a miniature inverted repeat transposable element (MITE) located upstream of the MYBE (Wang *et al.*, 2020). OsBAG4 functions as a bridge between OsSUVH7 and OsMYB106 to facilitate the binding of OsMYB106 to the consensus MYBE sequence in the *OsHKT1;5* promoter, thereby activating *OsHKT1;5* expression. Thus, a novel transcriptional complex, consisting of a DNA methylation reader, a chaperone regulator and a transcription factor, regulates *OsHKT1;5* expression under salt stress. In the current study, we observed that the *OsHKT1;5* gene was downregulated, and H3K4me3 levels in the *OsHKT1;5* chromatin were decreased in *ossdg721* mutants. Further ChIP-qPCR analysis revealed that OsSDG721 binds to the *OsHKT1;5* chromatin. It is possible that OsSDG721 combines with the OsSUVH7–OsBAG4–OsMYB106 transcriptional module to participate in the transcriptional regulation of the *OsHKT1;5* gene. Further studies are needed to elucidate how OsSDG721 is recruited to the *OsHKT1;5* chromatin for the deposition of H3K4me3 mark.

Experimental procedures

Plant material, growth conditions and saline-alkaline treatment

Whole genome-scale activation tagging pools were established in *Oryza sativa* L. ssp. *japonica* cv. Kitaake through co-cultivation of calli with *Agrobacterium*, as described previously (Ozawa, 2009). Seeds of wild-type Kitaake, AC lines, *ossdg721* loss-of-function mutant lines, *ossdg721 osshkt1;5* double mutant lines and transgenic *OsSDG721OX* lines were sterilized, washed and cultured, as previously described (Yoshida, 1976). The hydroponic experiment was carried out in a growth chamber maintained at 28 °C day/25 °C night temperature, 14-h light/10-h dark photoperiod, approximately 70% relative humidity and 200 $\mu\text{mol photons m}^{-2} \text{s}^{-1}$ light intensity. To perform breeding experiments, seeds were sown in the field in Changchung (125°41'N, 43°82'E) under normal conditions. To perform the saline-alkaline stress treatment, seeds were grown hydroponically in Yoshida's culture solution for 4 weeks and then transferred to culture solution supplemented with 25 mM Na_2CO_3 (pH = 10.0) for 5 days (Oosthuizen and Greyling, 2001). After the saline-alkaline treatment, seedlings were transferred to Na_2CO_3 -free Yoshida's culture solution for recovery.

Plasmid construction

To generate *ossdg721* loss-of-function mutant lines and *ossdg721 osshkt1;5* double mutant lines, single guide RNAs (sgRNAs) were cloned into *pYLsgRNA-OsU6a* and *pYLsgRNA-OsU6b* plasmids using OsSDG721-CRISPR-F1/R1, OsSDG721-CRISPR-F2/R2, OsHKT1;5-CRISPR-F1/R1 and OsHKT1;5-CRISPR-F2/R2 primer pairs, as described previously (Ma and Liu, 2016). To generate the *OsSDG721_{pro}:GUS* construct, a 2000-bp fragment upstream of the *OsSDG721* start codon was amplified by PCR using the primer pair OsSDG721_{pro}-F/R and then cloned into the *pCAMBIA3301* binary vector. To determine the subcellular localization of OsSDG721, full-length *OsSDG721* CDS (minus the stop codon) was amplified and cloned into plasmid 326-GFP under the control of the CaMV 35S promoter using recombination via *XbaI* and *BamHI* restriction endonuclease sites (Liu *et al.*, 2018). To construct the *CsV_{pro}:OsSDG721-FLAG* plasmid for the generation of *OsSDG721OX* lines, full-length *OsSDG721* CDS was amplified and cloned into *pCsV1300*, containing a 3×FLAG tag, using recombination (Xu *et al.*, 2012). To construct the *OsSDG721_{pro}:OsSDG721-FLAG* plasmid for the generation of complementation lines (*Com#1* and *Com#2*), the *OsSDG721* gene (including the promoter region) was cloned into the *pCAMBIA1302* binary vector using the G-OsSDG721-F/R primer pair. To generate GST-OsSDG217 constructs, full length *OsSDG217* was amplified and recombined into the *pGEX-4T1* vector via *BamHI* and *EcoRI* sites. All primers used for plasmid construction are listed in Table S7.

Mutant isolation and generation of transgenic plants

The *ossdg721* and *osshkt1;5* single mutants and *ossdg721 osshkt1;5* double mutant were generated using the CRISPR/Cas9 technology (Ma and Liu, 2016). Briefly, *OsSDG721*- and *OsHKT1;5*-specific sgRNAs were designed online at <http://skl.scau.edu.cn/targetdesign/>, and each sgRNA cassette was separately cloned into *pYLCRISPR/Cas9P_{ubi}-H*. The resulting constructs were separately introduced into wild-type Kitaake or *ossdg721-1* plants via *Agrobacterium*-mediated transformation

(Lu *et al.*, 2017). The resulting plants were selected in Yoshida's culture solution supplemented with 50 mg L⁻¹ hygromycin, and all mutations were confirmed by Sanger sequencing. T1 seeds lacking hygromycin resistance were used for subsequent experiments. To generate *OsSDG721OX* or complementation lines (*Com#1* and *Com#2*), the *CsV_{pro}:OsSDG721-FLAG* or *OsSDG721_{pro}:OsSDG721-FLAG* construct was introduced into Kitaake or *ossdg721-1* background, respectively. Homozygous transgenic lines were identified by selection on media containing 50 mg L⁻¹ hygromycin (Chen *et al.*, 1998).

GUS staining and subcellular localization analysis

Histochemical GUS staining was performed with *OsSDG721_{pro}:GUS* transgenic plants, as previously described (Jefferson *et al.*, 1987; Nan *et al.*, 2020). To determine the subcellular localization of *OsSDG721*, protoplasts were isolated from the leaf sheath of 3-week-old seedlings grown under 12-h light/12-h dark photoperiod and co-transfected with *OsSDG721-GFP* and *NLS-RFP* constructs by polyethylene glycol (PEG)-mediated transfection (Zhang *et al.*, 2011). The protoplasts were cultured at room temperature for 12–16 h and then observed under a fluorescence microscope (Olympus).

Measurement of Na⁺ and K⁺ contents of shoots

Seedlings were grown in hydroponic culture solution for 4 weeks and then transferred to the same culture solution supplemented with or without 25 mM Na₂CO₃ (pH = 10.0) for 5 days. After the saline-alkaline stress treatment, rice seedlings were washed twice with deionized water and then dried at 55 °C for 3 days. The dried shoot samples were weighed, ground, resuspended in 10 mL of ultrapure water and boiled at 100 °C for 8 h. The Na⁺ and K⁺ concentrations in the solution were determined by atomic absorption spectrophotometry (Rus *et al.*, 2001; Zhang *et al.*, 2017).

NBT and DAB staining

Four-week-old seedlings were transferred to hydroponic culture solution supplemented without or with 25 mM Na₂CO₃ (pH = 10.0) for 24 h. To determine ROS levels, leaves were vacuum-infiltrated for 30 min and then submerged for 12 h in 10 mM potassium phosphate buffer (pH = 7.8) containing 0.05% NBT (w/v) and 10 mM NaN₃ or for 24 h in 0.1% DAB (pH = 5.8). The stained leaves were cleared in the destaining buffer (ethanol:lactic acid:glycerol = 3:1:1) to eliminate the background green color (Nguyen *et al.*, 2017).

RNA-seq

Total RNA was isolated from the roots and shoots of wild-type Kitaake and *ossdg721* mutant seedlings grown in Yoshida's culture solution supplemented with 25 mM Na₂CO₃ (pH = 10.0) for 0 or 6 h using the TRIzol reagent (Invitrogen, CA, USA). RNA-seq was performed, as described previously (Wang *et al.*, 2020). Briefly, approximately 3 mg of RNA isolated from each sample was used for library construction, and RNA-seq was performed using the Illumina HiSeq 2500 platform (Novogene, Beijing, China) in three biological replicates. Each sample generated approximately 4.0 Gb clean reads. Reads from each sample were trimmed, mapped and analysed using FASTX-Toolkit (version 0.0.13), TOPHAT v.2.1.0 (Trapnell *et al.*, 2009) and CUFFLINKS (<http://cole-trapnell-lab.github.io/cufflinks/cuffdiff/index.html>), respectively. The selected RNA-seq data were confirmed by RT-qPCR.

ChIP-qPCR assay

The ChIP assay was performed, as described previously (Li *et al.*, 2018; Liu *et al.*, 2019), with slight modifications. Briefly, 2-week-old *ossdg721* and *OsSDG721_{pro}:OsSDG721-FLAG* seedlings grown in Yoshida's culture solution treated with 25 mM Na₂CO₃ (pH = 10.0) for 0 h (mock treatment) or 6 h. After the saline-alkaline stress treatment, approximately 20 g of seedlings were harvested and ground to a fine powder. Subsequently, chromatin complexes were extracted from the samples and sheared to 500-bp fragments using FB120 Sonic Dismembrator (Fisher Scientific). Then, anti-H3K4me3 (ab8580; Abcam) or anti-FLAG (F1804; Sigma-Aldrich) antibody was added to the chromatin complexes, and the samples were incubated overnight at 4 °C on a rotatory shaker. Protein A-agarose beads (Merck Millipore) were added to the mixture, and the samples were incubated for another 60–90 min. The protein-DNA cross links were reversed by incubating the samples at 65 °C for 8 h, and the released DNA fragments were purified. The enrichment of immunoprecipitated DNA was evaluated by RT-qPCR, with *OsUBQ10* serving as a negative control. Primers used for RT-qPCR are listed in Table S7.

EMSA

The EMSA experiment were performed, as described previously (Gao *et al.*, 2020). GST-tag proteins were induced via the *Escherichia coli* BL21 (DE3) cell line and immobilized onto glutathione-sepharose beads (GE Healthcare). The purified protein was confirmed by SDS-PAGE and prepared for EMSA. DNA probes were synthesized and biotin-labelled at the 5'-end by Sangon Biotechnology. Recombinant proteins were incubated with double-stranded probes at 4 °C in binding buffer for 30 min and then transferred to a nylon membrane via wet transfer and detected according to the instructions provided with the Chemiluminescent EMSA Kit (GS009; Beyotime). Primers used for EMSA are listed in Table S7.

Acknowledgements

This research was supported by the National Natural Science Foundation of China (31971822 to Z.-Y.X. and 32001448 to Y. L.), the National Key Research and Development Program of China (2016YFD0102003 to Z.-Y.X.), the Excellent Youth Foundation of Jilin Province of China (20190103020JH awarded to Z.-Y.X.), the Fundamental Research Funds for the Central Universities (2412020QD020 to Y.L.) and the Next-Generation Bio-Green21 Program of Rural Development Administration (RDA) of the Republic of Korea (PJ015968 to D.-J. Y.).

Conflict of Interest

The authors have no conflict of interest to declare.

Author contributions

Z.-Y.X. conceptualized and supervised the research. Y.L. performed most of the biochemical and cell-based experiments. X.C. performed the physiological analyses of plants treated with saline-alkaline stresses. S.X. performed the physiological analyses of plants. T.Q. performed the *Agrobacterium*-mediated transformation experiment. D.C. generated mutant lines. W.C. performed RNA-seq and data analysis. M.L. performed molecular cloning. L.H., D.-J.Y. and B.L. provided helpful suggestions for

improving the manuscript. Z.-Y.X. wrote the manuscript. All authors reviewed, revised and approved the final manuscript.

Accession numbers

Data generated in this study have been deposited in the National Center for Biotechnology Information Sequence Read Archive (accession number: PRJNA698439).

References

- Alonso, J.M., Stepanova, A.N., Leisse, T.J., Kim, C.J., Chen, H., Shinn, P., Stevenson, D.K. *et al.* (2003) Genome-wide insertional mutagenesis of *Arabidopsis thaliana*. *Science*, **301**, 653–657.
- Avramova, Z. (2009) Evolution and pleiotropy of TRITHORAX function in *Arabidopsis*. *Int. J. Dev. Biol.*, **53**, 371–381.
- Chen, L., Marmey, P., Taylor, N.J., Brizard, J.-P., Espinoza, C., D'Cruz, P., Huet, H. *et al.* (1998) Expression and inheritance of multiple transgenes in rice plants. *Nat. Biotechnol.*, **16**, 1060–1064.
- Chen, S., Jin, W., Wang, M., Zhang, F., Zhou, J., Jia, Q., Wu, Y. *et al.* (2003) Distribution and characterization of over 1000 T-DNA tags in rice genome. *Plant J.*, **36**, 105–113.
- Chen, S.-H., Zhou, L.-J., Xu, P. and Xue, H.-W. (2018) SPOC domain-containing protein Leaf inclination3 interacts with LIP1 to regulate rice leaf inclination through auxin signaling. *PLoS Genet.*, **14**, e1007829.
- Chen, T., Tsujimoto, N. and Li, E. (2004) The PWWP domain of Dnmt3a and Dnmt3b is required for directing DNA methylation to the major satellite repeats at pericentric heterochromatin. *Mol. Cell. Biol.*, **24**, 9048–9058.
- Cheng, R., Zhu, H., Cheng, X., Shutes, B. and Yan, B. (2020) Saline and Alkaline Tolerance of Wetland Plants—What are the Most Representative Evaluation Indicators?. *Sustainability*, **12**, 1913. <https://doi.org/10.3390/su12051913>
- Ding, Y., Wang, X., Su, L., Zhai, J., Cao, S., Zhang, D., Liu, C. *et al.* (2007) SDG714, a histone H3K9 methyltransferase, is involved in Tos17 DNA methylation and transposition in rice. *Plant Cell*, **19**, 9–22.
- van Enckevort, L.E.J., Droc, G., Piffanelli, P., Greco, R., Gagneur, C., Weber, C., González, V.M. *et al.* (2005) EU-OSTID: a collection of transposon insertional mutants for functional genomics in rice. *Plant Mol. Biol.*, **59**, 99–110.
- Gao, Y., Xu, Z., Zhang, L., Li, S., Wang, S., Yang, H., Liu, X. *et al.* (2020) MYB61 is regulated by GRF4 and promotes nitrogen utilization and biomass production in rice. *Nat. Commun.*, **11**, 1–12.
- Gou, X. and Li, J. (2011) Activation tagging. In Wang, Z.Y. and Yang, Z. (eds.), *Plant Signalling Networks*, (pp. 117–133). New Jersey: Humana Press.
- Gross, B.L. and Zhao, Z. (2014) Archaeological and genetic insights into the origins of domesticated rice. *Proc. Natl Acad. Sci.*, **111**, 6190–6197.
- Hauser, F. and Horie, T. (2010) A conserved primary salt tolerance mechanism mediated by HKT transporters: a mechanism for sodium exclusion and maintenance of high K⁺/Na⁺ ratio in leaves during salinity stress. *Plant, Cell & Environment*, **33**, 552–565.
- Henry, I.M., Nagalakshmi, U., Lieberman, M.C., Ngo, K.J., Krasileva, K.V., Vasquez-Gross, H., Akhunova, A. *et al.* (2014) Efficient genome-wide detection and cataloging of EMS-induced mutations using exome capture and next-generation sequencing. *Plant Cell*, **26**, 1382–1397.
- Horie, T., Hauser, F. and Schroeder, J. I. (2009) HKT transporter-mediated salinity resistance mechanisms in *Arabidopsis* and monocot crop plants. *Trends in Plant Science*, **14**, 660–668.
- Hsing, Y.-I., Chern, C.-G., Fan, M.-J., Lu, P.-C., Chen, K.-T., Lo, S.-F., Sun, P.-K. *et al.* (2007) A rice gene activation/knockout mutant resource for high throughput functional genomics. *Plant Mol. Biol.*, **63**, 351–364.
- Izawa, T. and Shimamoto, K. (1996) Becoming a model plant: The importance of rice to plant science. *Trends in Plant Science*, **1**, 95–99. [https://doi.org/10.1016/S1360-1385\(96\)80041-0](https://doi.org/10.1016/S1360-1385(96)80041-0)
- Jefferson, R.A., Kavanagh, T.A. and Bevan, M.W. (1987) GUS fusions: beta-glucuronidase as a sensitive and versatile gene fusion marker in higher plants. *The EMBO journal*, **6**, 3901–3907.
- Jeon, J.S., Lee, S., Jung, K.H., Jun, S.H., Jeong, D.H., Lee, J., Kim, C. *et al.* (2000) T-DNA insertional mutagenesis for functional genomics in rice. *Plant J.*, **22**, 561–570.
- Jeong, D.-H., An, S., Kang, H.-G., Moon, S., Han, J.-J., Park, S., Lee, H.S. *et al.* (2002) T-DNA insertional mutagenesis for activation tagging in rice. *Plant Physiol.*, **130**, 1636–1644.
- Jeong, D.H., An, S., Park, S., Kang, H.G., Park, G.G., Kim, S.R., Sim, J. *et al.* (2006) Generation of a flanking sequence-tag database for activation-tagging lines in japonica rice. *Plant J.*, **45**, 123–132.
- Jiang, P., Wang, S., Ikram, A.U., Xu, Z., Jiang, H., Cheng, B. and Ding, Y. (2018) SDG721 and SDG705 are required for rice growth. *J. Integr. Plant Biol.*, **60**, 530–535.
- Jiang, W., Zhou, H., Bi, H., Fromm, M., Yang, B. and Weeks, D.P. (2013) Demonstration of CRISPR/Cas9/sgRNA-mediated targeted gene modification in *Arabidopsis*, tobacco, sorghum and rice. *Nucleic Acids Res.*, **41**, e188.
- Kingston, R.E. and Tamkun, J.W. (2014) Transcriptional regulation by trithorax-group proteins. *Cold Spring Harbor perspectives in biology*, **6**, a019349.
- Kolesnik, T., Szeverenyi, I., Bachmann, D., Kumar, C.S., Jiang, S., Ramamoorthy, R., Cai, M. *et al.* (2004) Establishing an efficient Ac/Ds tagging system in rice: large-scale analysis of Ds flanking sequences. *Plant J.*, **37**, 301–314.
- Krajewski, W.A., Nakamura, T., Mazo, A. and Canaani, E. (2005) A motif within SET-domain proteins binds single-stranded nucleic acids and transcribed and supercoiled DNAs and can interfere with assembly of nucleosomes. *Mol. Cell. Biol.*, **25**, 1891–1899.
- Li, G., Chern, M., Jain, R., Martin, J.A., Schackwitz, W.S., Jiang, L., Vega-Sánchez, M.E. *et al.* (2016) Genome-wide sequencing of 41 rice (*Oryza sativa* L.) mutated lines reveals diverse mutations induced by fast-neutron irradiation. *Molecular Plant*, **9**, 1078–1081.
- Li, G., Jain, R., Chern, M., Pham, N.T., Martin, J.A., Wei, T., Schackwitz, W.S. *et al.* (2017) The sequences of 1504 mutants in the model rice variety Kitaake facilitate rapid functional genomic studies. *Plant Cell*, **29**, 1218–1231.
- Li, S., Tian, Y., Wu, K., Ye, Y., Yu, J., Zhang, J., Liu, Q. *et al.* (2018) Modulating plant growth-metabolism coordination for sustainable agriculture. *Nature*, **560**, 595–600.
- Li, T., Liu, B., Spalding, M.H., Weeks, D.P. and Yang, B. (2012) High-efficiency TALEN-based gene editing produces disease-resistant rice. *Nat. Biotechnol.*, **30**, 390.
- Liu, B., Liu, Y., Wang, B., Luo, Q., Shi, J., Gan, J., Shen, W.-H. *et al.* (2019) The transcription factor OsSUF4 interacts with SDG725 in promoting H3K36me3 establishment. *Nat. Commun.*, **10**, 1–14.
- Liu, B., Wei, G., Shi, J., Jin, J., Shen, T., Ni, T., Shen, W.H. *et al.* (2016) SET DOMAIN GROUP 708, a histone H3 lysine 36-specific methyltransferase, controls flowering time in rice (*Oryza sativa*). *New Phytol.*, **210**, 577–588.
- Liu, J., Guo, W. and Shi, D. (2010) Seed germination, seedling survival, and physiological response of sunflowers under saline and alkaline conditions. *Photosynthetica*, **48**, 278–286.
- Liu, K., Yu, Y., Dong, A. and Shen, W.H. (2017) SET DOMAIN GROUP701 encodes a H3K4-methyltransferase and regulates multiple key processes of rice plant development. *New Phytol.*, **215**, 609–623.
- Liu, Y., Zhang, A., Yin, H., Meng, Q., Yu, X., Huang, S., Wang, J. *et al.* (2018) Trithorax-group proteins ARABIDOPSIS TRITHORAX4 (ATX4) and ATX 5 function in abscisic acid and dehydration stress responses. *New Phytol.*, **217**, 1582–1597.
- Lu, Y., Ye, X., Guo, R., Huang, J., Wang, W., Tang, J., Tan, L. *et al.* (2017) Genome-wide targeted mutagenesis in rice using the CRISPR/Cas9 system. *Molecular plant*, **10**, 1242–1245.
- Lu, Z., Huang, X., Ouyang, Y. and Yao, J. (2013) Genome-wide identification, phylogenetic and co-expression analysis of OsSET gene family in rice. *PLoS One*, **8**, e65426.
- Ma, X., Zhang, Q., Zhu, Q., Liu, W., Chen, Y., Qiu, R., Wang, B., Yang, Z., Li, H., Lin, Y., Xie, Y., Shen, R., Chen, S., Wang, Z., Chen, Y., Guo, J., Chen, L., Zhao, X., Dong, Z. and Liu, Y.-G. (2015) A Robust CRISPR/Cas9 System for Convenient, High-Efficiency Multiplex Genome Editing in Monocot and Dicot Plants. *Molecular Plant*, **8**, 1274–1284.
- Ma, X. and Liu, Y. (2016) CRISPR/Cas9-based genome editing systems and the analysis of targeted genome mutations in plants. *Heredity*, **38**, 118–125. <https://doi.org/10.16288/j.ycz.15-395>

- Memelink, J. (2003) T-DNA activation tagging. In Grotewold, E. (ed.), *Plant Functional Genomics* (pp. 345–361). New Jersey: Humana Press. <https://doi.org/10.1385/1-59259-413-1:345>
- Miao, J., Guo, D., Zhang, J., Huang, Q., Qin, G., Zhang, X., Wan, J. et al. (2013) Targeted mutagenesis in rice using CRISPR-Cas system. *Cell Res.*, **23**, 1233–1236.
- Miyao, A., Tanaka, K., Murata, K., Sawaki, H., Takeda, S., Abe, K., Shinozuka, Y. et al. (2003) Target site specificity of the Tos17 retrotransposon shows a preference for insertion within genes and against insertion in retrotransposon-rich regions of the genome. *Plant Cell*, **15**, 1771–1780.
- Moscou, M.J. and Bogdanove, A.J. (2009) A simple cipher governs DNA recognition by TAL effectors. *Science*, **326**, 1501.
- Munns, R. and Tester, M. (2008) Mechanisms of Salinity Tolerance. *Annual Review of Plant Biology*, **59**, 651–681.
- Nan, N., Wang, J., Shi, Y., Qian, Y., Jiang, L., Huang, S., Liu, Y. et al. (2020) Rice plastidial NAD-dependent malate dehydrogenase 1 negatively regulates salt stress response by reducing the vitamin B6 content. *Plant Biotechnol. J.*, **18**, 172–184.
- Nguyen, H.M., Sako, K., Matsui, A., Suzuki, Y., Mostofa, M.G., Ha, C.V., Tanaka, M. et al. (2017) Ethanol enhances high-salinity stress tolerance by detoxifying reactive oxygen species in Arabidopsis thaliana and rice. *Frontiers in plant science*, **8**, 1001.
- Oosthuizen, M.M. and Greyling, D. (2001) Hydroxyl radical generation: the effect of bicarbonate, dioxygen and buffer concentration on pH-dependent chemiluminescence. *Redox Rep.*, **6**, 105–116.
- Østergaard, L. and Yanofsky, M.F. (2004) Establishing gene function by mutagenesis in *Arabidopsis thaliana*. *Plant J.*, **39**, 682–696.
- Ozawa, K. (2009) Establishment of a high efficiency Agrobacterium-mediated transformation system of rice (*Oryza sativa* L.). *Plant Sci.*, **176**(4), 522–527.
- Rus, A., Yokoi, S., Sharkhuu, A., Reddy, M., Lee, B.-H., Matsumoto, T.K., Koiwa, H. et al. (2001) AtHKT1 is a salt tolerance determinant that controls Na⁺ entry into plant roots. *Proc. Natl Acad. Sci.*, **98**, 14150–14155.
- Sallaud, C., Meynard, D., van Boxtel, J., Gay, C., Bès, M., Brizard, J. P., Larmande, P., Ortega, D., Raynal, M., Portefaix, M., Ouwerkerk, P. B. F., Rueb, S., Delseny, M. and Guiderdoni, E. (2003) Highly efficient production and characterization of T-DNA plants for rice (*Oryza sativa* L.) functional genomics. *Theoretical and Applied Genetics*, **106**, 1396–1408.
- Shahid, S.A., Zaman, M. and Heng, L. (2018) Soil salinity: historical perspectives and a world overview of the problem. In: Zaman, M., Shahid, S.A. and Heng, L. (eds.), *Guideline for salinity assessment, mitigation and adaptation using nuclear and related techniques* (pp. 43–53). Cham: Springer.
- Sharma, P., Jha, A.B., Dubey, R.S. and Pessarakli, M. (2012) Reactive oxygen species, oxidative damage, and antioxidative defense mechanism in plants under stressful conditions. *J. Bot.*, **2012**, 1–26.
- Shrivastava, P. and Kumar, R. (2015) Soil salinity: A serious environmental issue and plant growth promoting bacteria as one of the tools for its alleviation. *Saudi J. Biol. Sci.*, **22**, 123–131.
- Si, L., Chen, J., Huang, X., Gong, H., Luo, J., Hou, Q., Zhou, T. et al. (2016) OsSPL13 controls grain size in cultivated rice. *Nat. Genet.*, **48**, 447–456.
- Sun, C., Fang, J., Zhao, T., Xu, B., Zhang, F., Liu, L., Tang, J. et al. (2012) The histone methyltransferase SDG724 mediates H3K36me2/3 deposition at MADS50 and RFT1 and promotes flowering in rice. *Plant Cell*, **24**, 3235–3247.
- Tang, L., Cai, H., Zhai, H., Luo, X., Wang, Z., Cui, L. and Bai, X. (2014) Overexpression of Glycine soja WRKY20 enhances both drought and salt tolerance in transgenic alfalfa (*Medicago sativa* L.). *Plant Cell, Tissue and Organ Culture (PCTOC)*, **118**, 77–86.
- Trapnell, C., Pachter, L. and Salzberg, S.L. (2009) TopHat: discovering splice junctions with RNA-Seq. *Bioinformatics*, **25**, 1105–1111.
- Wan, S., Wu, J., Zhang, Z., Sun, X., Lv, Y., Gao, C., Ning, Y. et al. (2009) Activation tagging, an efficient tool for functional analysis of the rice genome. *Plant Mol. Biol.*, **69**, 69–80.
- Wang, J., Nan, N., Li, N., Liu, Y., Wang, T.-J., Hwang, I., Liu, B. and et al. (2020) A DNA Methylation Reader-Chaperone Regulator-Transcription Factor Complex Activates OsHKT1; 5 Expression during Salinity Stress. *Plant Cell*, **32**, 3535–3558.
- Wang, L., Zheng, J., Luo, Y., Xu, T., Zhang, Q., Zhang, L., Xu, M., Wan, J., Wang, M., Zhang, C. and Fan, Y. (2013) Construction of a genomewide RNAi mutant library in rice. *Plant Biotechnology Journal*, **11**, 997–1005.
- Wang, N., Long, T., Yao, W., Xiong, L., Zhang, Q. and Wu, C. (2013) Mutant Resources for the Functional Analysis of the Rice Genome. *Molecular Plant*, **6**, 596–604.
- Wei, F.-J., Droc, G., Guiderdoni, E. and Yue-ie, C.H. (2013) International consortium of rice mutagenesis: resources and beyond. *Rice*, **6**, 1–12.
- Weigel, D., Ahn, J.H., Blázquez, M.A., Borevitz, J.O., Christensen, S.K., Fankhauser, C., Ferrández, C. et al. (2000) Activation tagging in Arabidopsis. *Plant Physiol.*, **122**, 1003–1014.
- Wu, C., Li, X., Yuan, W., Chen, G., Kilian, A., Li, J., Xu, C. et al. (2003) Development of enhancer trap lines for functional analysis of the rice genome. *Plant J.*, **35**, 418–427.
- Xie, K., Minkenberg, B. and Yang, Y. (2015) Boosting CRISPR/Cas9 multiplex editing capability with the endogenous tRNA-processing system. *Proc. Natl Acad. Sci.*, **112**, 3570–3575.
- Xu, Z.-Y., Lee, K.H., Dong, T., Jeong, J.C., Jin, J.B., Kanno, Y., Kim, D.H., Kim, S. Y., Seo, M., Bressan, R. A., Yun D.-J. and Hwang, I. (2012) A Vacuolar β -Glucosidase Homolog That Possesses Glucose-Conjugated Absciscic Acid Hydrolyzing Activity Plays an Important Role in Osmotic Stress Responses in Arabidopsis. *The Plant Cell*, **24**, 2184–2199.
- Yoshida, S. (1976) Routine procedure for growing rice plants in culture solution. In Yoshida, S., Forno, D.A., Cock, J.H. and Gomez, K.A. (eds.), *Laboratory manual for physiological studies of rice* (pp. 61–66). Philippines: International Rice Research.
- Yuan, H., Qin, P., Hu, L., Zhan, S., Wang, S., Gao, P., Li, J. et al. (2019) OsSPL18 controls grain weight and grain number in rice. *Journal of Genetics and Genomics*, **46**, 41–51.
- Zhang, H., Liu, X.-L., Zhang, R.-X., Yuan, H.-Y., Wang, M.-M., Yang, H.-Y., Ma, H.-Y. et al. (2017) Root damage under alkaline stress is associated with reactive oxygen species accumulation in rice (*Oryza sativa* L.). *Front. Plant Sci.*, **8**, 1580.
- Zhang, Y., Su, J., Duan, S., Ao, Y., Dai, J., Liu, J., Wang, P. et al. (2011) A highly efficient rice green tissue protoplast system for transient gene expression and studying light/chloroplast-related processes. *Plant methods*, **7**, 1–14.

Supporting information

Additional supporting information may be found online in the Supporting Information section at the end of the article.

Figure S1. Identification of activation-tagged lines based on the detection of green fluorescent protein (GFP) signal.

Figure S2. Agronomic traits of *OsSDG721* overexpression (*OsSDG721OX*) lines.

Figure S3. Tissue-specific expression patterns of *OsSDG721*, and subcellular localization of *OsSDG721*.

Figure S4. Generation of loss-of-function *ossdg721* mutants.

Figure S5. Ion contents in the roots of different genotypes.

Figure S6. Examination of H3K4 methyltransferase activity.

Figure S7. *OsSDG721* affects the transcriptional landscape in rice under saline–alkaline stress conditions.

Figure S8. Image of EMSA.

Table S1. List of differentially expressed genes (DEGs) in shoot in *ossdg721-1* vs. Kitaake under normal condition.

Table S2. List of differentially expressed genes (DEGs) in root in *ossdg721-1* vs. Kitaake under normal condition.

Table S3. List of differentially expressed genes (DEGs) in shoot in *ossdg721-1* vs. Kitaake under saline–alkaline condition.

Table S4. List of differentially expressed genes (DEGs) in root in *ossdg721-1* vs. Kitaake under saline–alkaline condition.

Table S5. List of saline–alkaline stress responsive genes in Kitaake.

Table S6. List of saline–alkaline responsive genes affected by *OsSDG721*.

Table S7. List of primers used in this study.